

Title	Crystal defect topography of Stranski-Krastanow quantum dots by atomic force microscopy
Authors	Gradkowski, Kamil;Sadler, Thomas C.;Merani, Lorenzo O.;Dimastrodonato, Valeria;Parbrook, Peter J.;Huyet, Guillaume;Pelucchi, Emanuele
Publication date	2010
Original Citation	Gradkowski, K., Sadler, T. C., Merani, L. O., Dimastrodonato, V., Parbrook, P. J., Huyet, G. and Pelucchi, E. (2010) 'Crystal defect topography of Stranski-Krastanow quantum dots by atomic force microscopy', Applied Physics Letters, 97(19), pp. 191106. doi: 10.1063/1.3514237
Type of publication	Article (peer-reviewed)
Link to publisher's version	<a href="http://aip.scitation.org/doi/abs/10.1063/1.3514237">http://aip.scitation.org/doi/abs/10.1063/1.3514237</a> - 10.1063/1.3514237
Rights	© 2010 American Institute of Physics. This article may be downloaded for personal use only. Any other use requires prior permission of the author and AIP Publishing. The following article appeared in Gradkowski, K., Sadler, T. C., Merani, L. O., Dimastrodonato, V., Parbrook, P. J., Huyet, G. and Pelucchi, E. (2010) 'Crystal defect topography of Stranski-Krastanow quantum dots by atomic force microscopy', Applied Physics Letters, 97(19), pp. 191106 and may be found at <a href="http://aip.scitation.org/doi/abs/10.1063/1.3514237">http://aip.scitation.org/doi/abs/10.1063/1.3514237</a>
Download date	2025-06-10 04:54:10
Item downloaded from	<a href="https://hdl.handle.net/10468/4328">https://hdl.handle.net/10468/4328</a>



**University College Cork, Ireland**  
Coláiste na hOllscoile Corcaigh

# Crystal defect topography of Stranski–Krastanow quantum dots by atomic force microscopy

K. Gradkowski, T. C. Sadler, L. O. Mereni, V. Dimastrodonato, P. J. Parbrook, G. Huyet, and E. Pelucchi<sup>\*</sup>

Citation: *Appl. Phys. Lett.* **97**, 191106 (2010); doi: 10.1063/1.3514237

View online: <http://dx.doi.org/10.1063/1.3514237>

View Table of Contents: <http://aip.scitation.org/toc/apl/97/19>

Published by the [American Institute of Physics](#)

---

---



# Crystal defect topography of Stranski–Krastanow quantum dots by atomic force microscopy

K. Gradkowski,<sup>1,2</sup> T. C. Sadler,<sup>3</sup> L. O. Mereni,<sup>1</sup> V. Dimastrodonato,<sup>1</sup> P. J. Parbrook,<sup>1,4</sup>  
G. Huyet,<sup>1,2</sup> and E. Pelucchi<sup>1,a)</sup>

<sup>1</sup>Tyndall National Institute, University College Cork, Cork, Ireland

<sup>2</sup>Centre for Advanced Photonics and Process Analysis, Cork Institute of Technology, Cork, Ireland

<sup>3</sup>Department of Materials Science and Metallurgy, University of Cambridge, Cambridge CB2 3QZ, England

<sup>4</sup>Department of Electrical and Electronic Engineering, University College Cork, Cork, Ireland

(Received 10 September 2010; accepted 20 October 2010; published online 8 November 2010)

We demonstrate a technique to monitor the defect density in capped quantum dot (QD) structures by performing an atomic force microscopy (AFM) of the final surface. Using this method we are able to correlate their density with the optical properties of the dot structures grown at different temperatures. Parallel transmission electron microscopy analysis shows that the AFM features are directly correlated with the density of stacking faults that originate from abnormally large dots. The technique is rapid and noninvasive making it an ideal diagnostic tool for optimizing the parameters of practical QD-based devices. © 2010 American Institute of Physics. [doi:10.1063/1.3514237]

Semiconductor quantum dots (QDs) are an important technology for a wide variety of optoelectronic device applications. A further growing field of interest is that of low-density QD arrays for quantum information.<sup>1–3</sup> In contrast, laser and amplifier applications require high dot density and uniformity to reduce threshold and improve gain. This is generally obtained by utilizing a self-assembled, Stranski–Krastanov (SK) growth mode. To produce such dots, there are two main techniques: molecular beam epitaxy (MBE) and metal-organic vapor phase epitaxy (MOVPE); together with others which can be considered permutations of these two. In general, MOVPE has struggled to catch-up with MBE results, where several groups have reported  $>1.3\ \mu\text{m}$  laser action using In(Ga)As/GaAs QDs,<sup>4–6</sup> whereas for MOVPE good laser properties at wavelengths approaching  $1.3\ \mu\text{m}$  have been attained by very few groups, with a single recent report of a MOVPE dot laser having achieved this wavelength (see Ref. 7 and references therein). Moreover, the MOVPE literature presents a variety of growth recipes which should bring similar results but are practically very different (growth temperature [T], growth interruptions, V/III ratio). As a result there is still no easy and straightforward path to reproducible high-quality dots and correspondent laser action. It should be noted that growth by MOVPE is additionally peculiar, because it involves decomposition of the precursor species at the growing surface, resulting in a complex evolution of the surface features, e.g., differently organized step-bunching.<sup>8</sup>

It is an important pre-requisite for the QD layers (for example in a laser structure) to be “effectively” *defect-free*, otherwise the device electrical and optical performance will be degraded. There are few techniques that enable evaluation of the defect density present in a QD sample. The most popular is transmission electron microscopy (TEM),<sup>9</sup> which is expensive, time-consuming, and most importantly destructive, making it ill-suited for performing measurements on a future device structure. Other microscopic techniques, such as an atomic force microscopy (AFM), have been mostly em-

ployed to measure uncapped QDs; to determine their size, shape, and density. However, for device structures the dots must be capped, often at higher T, which can change their physical, and hence optical, properties. This makes the observation of the QD layer properties and possible defect formation very difficult without TEM.

AFM is a standard tool in GaN analysis, where it is employed to detect the threading dislocations density in an epitaxial layer.<sup>10</sup> In this paper we show that defects induced by nonoptimal InAs/GaAs QDs can be observed by AFM allowing the density of *threading* defects to be determined without recourse to TEM (used here only to confirm our findings). Additionally we can unambiguously correlate our structural analysis with the optical properties of the sample under investigation. These results are coherent with the observations of a number of other groups obtained by TEM (Ref. 9) or by uncapped AFM (Ref. 11) analysis, and are relevant as a tool for reducing the appearance of large, defected QDs, the presence of which is very often described in the literature.<sup>11,12</sup>

A series of photoluminescence (PL) QD structures were prepared at various temperatures ( $T_{\text{QD}}$ ), ranging from 475 to 550 °C. The structures were grown on (001) GaAs substrates misoriented 0.2° toward (111)A. In the middle of the 300 nm GaAs buffer layer an  $\text{Al}_{0.3}\text{Ga}_{0.7}\text{As}$  barrier was inserted for calibration purposes, both grown at an estimated surface temperature of 690 °C and growth rate of  $1\ \mu\text{m/h}$ . The precursors were trimethylgallium (TMGa), trimethylaluminum (TMA1), and arsine ( $\text{AsH}_3$ ). For the dots trimethylindium and tertiarybutylarsine (TBA) were used<sup>7,13</sup> with a growth rate of 0.022 ML/s and V/III ratio of 0.44. To maintain control of the low V/III ratio an arsenic interruption method, similar to that of Lee *et al.*,<sup>14</sup> was implemented. The nominal InAs thickness was 1.7 ML. After a 60 s interruption the dots were capped using a two-step process: first 50 nm was grown using TBAs and TMGa at the same temperature as the dots, at a rate of  $0.25\ \mu\text{m/h}$  and V/III ratio of 15. Then, for the final 250 nm, the temperature of the growth was increased to 570 °C, while the rest of the parameters were as for the buffer layer below the QDs. No additional

<sup>a)</sup>Electronic mail: emanuele.pelucchi@tyndall.ie.

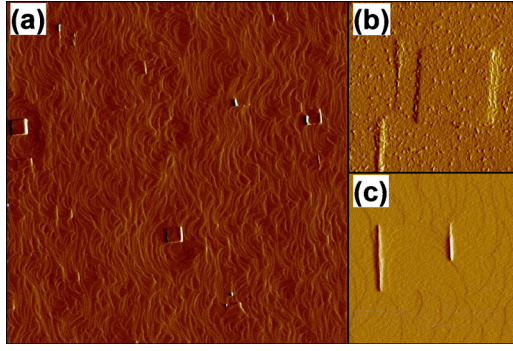


FIG. 1. (Color online) AFM image (signal amplitudes) of the top surface of the QD structure grown at low  $T_{\text{QD}}$ . (a)  $10 \times 10 \mu\text{m}^2$  scan area shows a large number of square defects. (b) and (c) depict  $1 \times 1 \mu\text{m}^2$  zoom-in on the defects.

optimization techniques, such as capping with a strain-relief-layer or annealing, were employed to improve the quality of the dots/surface. The structures were examined using AFM and room-T PL with 1 mW excitation from a He-Ne laser operating at 633 nm.

Figure 1(a) shows a representative  $10 \times 10 \mu\text{m}^2$  AFM micrograph of the top surface of the structure grown at  $475^\circ\text{C}$ . The sample was grown at slightly different growth conditions from the PL samples, and was designed to highlight structural features. In addition to a general bunching of atomic steps, a number of square and line features are observed, which can be seen in more detail in the  $1 \times 1 \mu\text{m}^2$  images in Figs. 1(b) and 1(c). The features appear as inverted plateaus (“playas”) on the surface and are several nanometers in amplitude. They can have well-defined edges or appear to be partially filled. They are highly symmetric and their size is extremely regular, around 440 nm. Discussion later in this paper will support our assertion that these features are the result of extended defects nucleated at the QD layer, which then thread up to the surface through the cap layer, consistent with other reports.<sup>12</sup>

The density of the surface defects as a function of QD growth temperature is presented in Fig. 2 for the PL samples. The insets show the corresponding AFM micrographs.

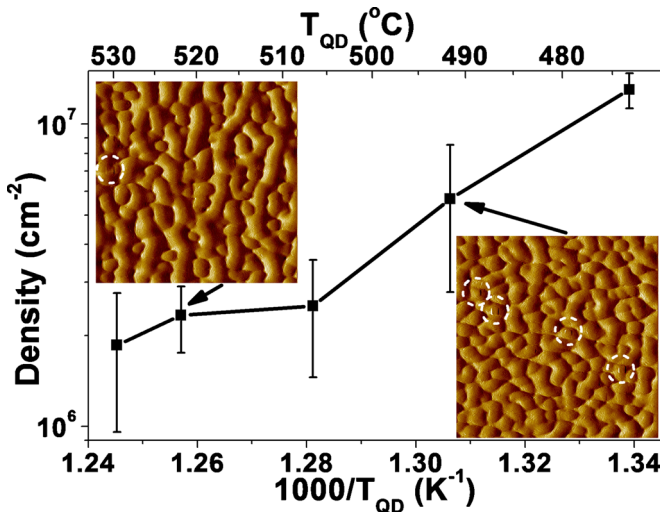


FIG. 2. (Color online) Dependence of the surface defect density on the QD growth temperature. The insets show  $10 \times 10 \mu\text{m}^2$  AFM scans for selected values of  $T_{\text{QD}}$  with circles indicating the position of the surface defects.

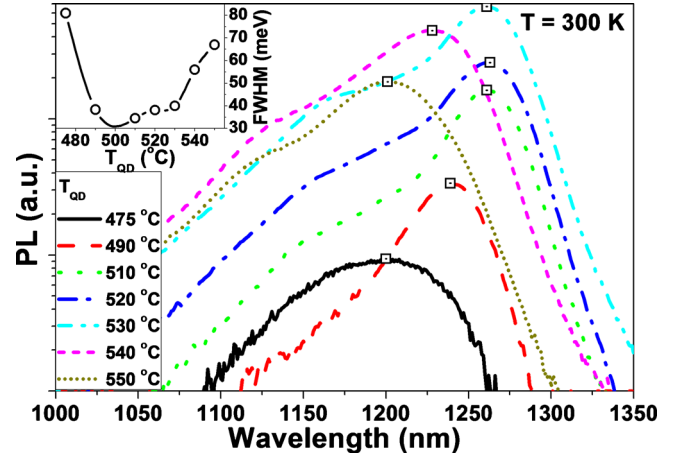


FIG. 3. (Color online) Dependence of the PL spectrum on the growth temperature of the QDs. Dots represent the maximum of the ground state emission. The inset shows dependence of the FWHM on the QD growth temperature.

With increasing  $T_{\text{QD}}$  the density of the defects drops from  $1.3 \times 10^7 \text{ cm}^{-2}$  for the dots grown at  $475^\circ\text{C}$  to  $1.85 \times 10^6 \text{ cm}^{-2}$  for  $T_{\text{QD}}=530^\circ\text{C}$ . For the structures grown at even higher temperatures, the defect density was lower than our detection limit of  $\sim 1 \times 10^6 \text{ cm}^{-2}$ . This limit is simply related to the area sampled and can be lowered at a cost in examination time. Despite the limited temperature range investigated we observe that the plot might suggest that there is not a single activation energy for the processes responsible for the defect formation, or more precisely their extinction.

The observed defect density has been correlated with the luminescent properties of the structures, shown in Fig. 3. As  $T_{\text{QD}}$  increases from  $475$  to  $530^\circ\text{C}$ , a rapid increase in intensity, by two orders of magnitude, is accompanied by a narrowing of the PL full-width at half-maximum (FWHM) and a redshift in the luminescence peak. The initial change in FWHM and redshift is extremely rapid with the FWHM falling from 80 meV at  $475^\circ\text{C}$  to below 40 meV for all other temperatures in this range (see inset in Fig. 3). The luminescence peak shifts from 1200 nm at  $475^\circ\text{C}$  and saturates around 1260 nm at  $510^\circ\text{C}$ . For  $T_{\text{QD}} > 530^\circ\text{C}$  the spectra undergo a blueshift (down to 1200 nm ground state emission), become much broader (with  $\text{FWHM}=67 \text{ meV}$  for  $T_{\text{QD}}=550^\circ\text{C}$ ), and the luminescence intensity decreases. We associate this effect with *in situ* annealing of the QDs at the higher growth temperature.<sup>15</sup> In this regime we do not observe surface defects.

It is notable that the playas have, within statistical error, the same dimension, which implies a common depth of nucleation of the feature, supposedly the QD layer. One defect that can lead to such geometric shapes are a set of stacking faults (SFs) nucleated at a common point (or apex) bounded by four stair-rod dislocations and propagating out as a square pyramid in the subsequent overgrowth. Such defects have been reported previously in TEM studies for both III-V QDs (Ref. 12) and growth of ZnSe on GaAs.<sup>16</sup> A SF is a defect in the cubic stacking of the crystal in the  $\{111\}$  plane, at its simplest being a layer of hexagonally stacked (wurtzite) material in the zinc-blende structure. While not in itself a nonradiative center, the partial dislocations bounding it provide a route for nonradiative recombination.



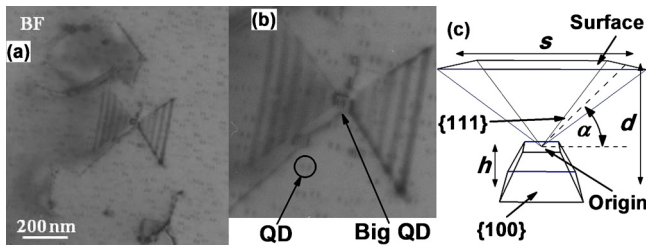


FIG. 4. (Color online) (a)  $1 \times 1 \mu\text{m}^2$  220 bright field TEM micrograph of the PL structure grown at  $510^\circ\text{C}$ . (b) Zoom-in on the SF depicting a big QD as a source of the defect. Small interference patterns correspond to normal dots. (c) Schematic of the origin of the surface square defects and method of calculation of the SF origin depth.

To confirm this we have performed preliminary TEM analysis on the QD structure grown at  $510^\circ\text{C}$ , using a Philips CM30 operated at 300 kV. For this purpose, plan view samples were prepared by grinding and polishing to  $\sim 30 \mu\text{m}$  and then thinned to electron transparency using a Gatan precision ion polishing system. The 220 bright-field TEM micrograph, presented in Fig. 4(a), clearly shows SFs. The size of the defects is comparable to that observed by AFM and their density, determined by more extensive imaging of the sample, is around  $1.7 \times 10^7 \text{ cm}^{-2}$  (the good dot density is  $\sim 3.31 \times 10^{10} \text{ cm}^{-2}$ , as estimated by the number of small interference patterns in the TEM micrograph, which corroborates the PL results indicating the structure was grown under near-ideal conditions), which is consistent with the data in Fig. 2 and further supports our assertion that the surface features are the result of SF arising from the dot layer. In Fig. 4(b) an interference pattern at the apex of the SF is observed. This may be associated with an abnormally big dot,<sup>17</sup> suggesting that is the SF source.

The SF will propagate along the four {111} planes from its source. If there is no interaction with another defect they will propagate to the surface. The small stacking change on the four {111} planes meeting the {001} surface will leave a square feature observable by AFM due to the (equal and opposite) out-of-growth-plane components of the Burgers vectors terminating the SF at each end, which may be enhanced by growth effects [Fig. 4(c)]. Assuming that the SF defects are formed at a constant depth in the film, the surface defect squares will be a constant size. Computing the angle between the {111} SF plane and the growth plane, with the apex of the four stair-rod dislocations occurring on the top of the QD, then the thickness of the capping layer,  $d$ , can be calculated from Eq. (1) below, where the variables are as defined in Fig. 4(c)

$$d = \frac{s \tan \alpha + 2h}{2}. \quad (1)$$

From geometry  $\alpha = 54.7^\circ$ ,<sup>18</sup>  $s$  was determined above to be 440 nm, and we assume the large dot height,  $h$ , to be 10 nm. This gives  $d = 320 \text{ nm}$ , close to the 300 nm nominal capping thickness.

We have so far concentrated on the square features. A number of lines are also found by AFM. The longest match the length of the edges of the square, and are likely a single SF bounded by two Shockley partial dislocations.<sup>16</sup> Shorter lines are also observed, which require further investigation to

determine if the surface feature has been partially masked, or whether other mechanisms may be responsible. The TEM images show a number of unidentified defect structures in the sample, and their analysis will be the subject of future work.

In conclusion, we have demonstrated a technique to monitor the defect density in capped QD samples by performing an AFM scan of the final surface. We were able to correlate their density with the optical properties of the dot structures grown at different temperatures while TEM analysis showed that the AFM features are directly correlated with the density of SF (and presumably abnormally large dots) in the samples. The technique is rapid and noninvasive making it an ideal diagnostic tool.

This work was conducted under the framework of the INSPIRE programme, funded by the Irish Government's Programme for Research in Third Level Institutions, Cycle 4, National Development Plan 2007-2013, and funded by Science Foundation Ireland (SFI) under Grant No. 05/IN.1/I25. PJP acknowledges financial support from SFI Engineering Professorships scheme (07/EN/E001a). T.C.S. acknowledges funding from an EPSRC PhD-Plus Fellowship. The authors are grateful to Dr. K. Thomas for MOVPE system support.

<sup>1</sup>R. J. Young, S. J. Dewhurst, R. M. Stevenson, A. J. Shields, P. Atkinson, K. Cooper, and D. A. Ritchie, *Appl. Phys. Lett.* **91**, 011114 (2007).

<sup>2</sup>L. O. Mereni, V. Dimastrodonato, R. J. Young, and E. Pelucchi, *Appl. Phys. Lett.* **94**, 223121 (2009).

<sup>3</sup>F. Chi, X.-N. Dai, and L.-L. Sun, *Appl. Phys. Lett.* **96**, 082102 (2010).

<sup>4</sup>D. L. Huffaker, G. Park, Z. Zou, O. B. Shchenkin, and D. G. Deppe, *Appl. Phys. Lett.* **73**, 2564 (1998).

<sup>5</sup>S. Ghosh, S. Pradhan, and P. Bhattacharya, *Appl. Phys. Lett.* **81**, 3055 (2002).

<sup>6</sup>A. Salhi, G. Rainò, L. Fortunato, V. Tasco, L. Martiradonna, M. T. Todaro, M. De Giorgi, R. Cingolani, A. Passaseo, E. Luna, A. Trampert, and M. De Vittorio, *Nanotechnology* **19**, 275401 (2008).

<sup>7</sup>D. Guimard, M. Ishida, D. Bordel, L. Li, M. Nishioka, Y. Tanaka, M. Ekawa, H. Sudo, T. Yamamoto, H. Kondo, M. Sugawara, and Y. Arakawa, *Nanotechnology* **21**, 105604 (2010).

<sup>8</sup>E. Pelucchi, N. Moret, B. Dwir, D. Y. Oberli, A. Rudra, N. Gogneau, A. Kumar, E. Kapon, E. Levy, and A. Palevski, *J. Appl. Phys.* **99**, 093515 (2006); A. Dalla Volta, D. D. Vvedensky, N. Gogneau, E. Pelucchi, A. Rudra, B. Dwir, E. Kapon, and C. Ratsch, *Appl. Phys. Lett.* **88**, 203104 (2006).

<sup>9</sup>K. Stewart, M. Buda, J. Wong-Leung, L. Fu, C. Jagadish, A. Stiff-Roberts, and P. Bhattacharya, *J. Appl. Phys.* **94**, 5283 (2003).

<sup>10</sup>See, for example, S. E. Bennett, D. Holec, M. J. Kappers, C. J. Humphreys, and R. A. Oliver, *Rev. Sci. Instrum.* **81**, 063701 (2010); P. Makaram, J. Joh, J. A. del Alamo, T. Palacios, and C. V. Thompson, *Appl. Phys. Lett.* **96**, 233509 (2010).

<sup>11</sup>D. Guimard, M. Nishioka, S. Tsukamoto, and Y. Arakawa, *J. Cryst. Growth* **298**, 548 (2007).

<sup>12</sup>K. Sears, J. Wong-Leung, H. H. Tan, and C. Jagadish, *J. Appl. Phys.* **99**, 113503 (2006).

<sup>13</sup>D. Guimard, M. Ishida, L. Li, M. Nishioka, Y. Tanaka, H. Sudo, T. Yamamoto, H. Kondo, M. Sugawara, and Y. Arakawa, *Appl. Phys. Lett.* **94**, 103116 (2009).

<sup>14</sup>Y. Lee, E. Ahn, J. Kim, P. Moon, C. Yang, E. Yoon, H. Lim, and H. Cheong, *Appl. Phys. Lett.* **90**, 033105 (2007).

<sup>15</sup>S. Liang, H. L. Zhu, X. L. Ye, and W. Wang, *J. Cryst. Growth* **311**, 2281 (2009).

<sup>16</sup>N. Wang, I. K. Sou, and K. K. Fung, *J. Appl. Phys.* **80**, 5506 (1996).

<sup>17</sup>A. M. Sanchez, R. Beanland, N. F. Hasbullah, M. Hopkinson, and J. P. R. David, *J. Appl. Phys.* **106**, 024502 (2009).

<sup>18</sup>P. J. C. King, M. B. H. Breese, P. R. Wilshaw, and G. W. Grime, *Phys. Rev. B* **51**, 2732 (1995).